J Therm Anal Calorim (2016) 123:2599–2610
DOI 10.1007/s10973-016-5244-x

Approximation-based integral versus differential isoconversional approaches to the evaluation of kinetic parameters from thermogravimetry

kinetic analysis of the dehydration of a pharmaceutical hydrate

R. Neglur[1] · D. Grooff[1] · E. Hosten[1] · M. Aucamp[2] · W. Liebenberg[2]

Received: 25 September 2015 / Accepted: 8 January 2016 / Published online: 28 January 2016

Abstract The relative accuracies of approximation-based integral versus differential isoconversional approaches for 'actual' E determination were investigated on experimental dehydration data of roxithromycin monohydrate from thermogravimetric (TG) analysis. The dehydration kinetic parameters and the relationship to the structural characteristics of the monohydrate and anhydrate forms from differential scanning calorimetry (DSC) and single-crystal X-ray diffractometry (SC-XRD) are also reported. Integral methods versus the differential Friedman isoconversional method evaluated E correspondences in both iso- and non-isothermal TG methods. The reliability in E from Friedman approached that of estimates from current most accepted integral isoconversional methods and was even superior to methods (for non-isothermal studies) that employ an approximation to the temperature integral (modified Kissinger–Akahira–Sunose, Senum–Yang fourth degree). Structural characterization (DSC, SC-XRD) and kinetic analysis from generalized kinetic master plots concluded that coordinated water occupied interlinked voids in crystal structure which may have facilitated the multidimensional diffusional loss of water upon heating without disruption of the crystal structure.

Keywords Roxithromycin · Solid-state kinetics · Advanced isoconversional · Differential Friedman

Introduction

Solid-state processes that involve a change in mass can be and are often followed by thermogravimetric (TG) analysis and when used to investigate reaction kinetics, usually report kinetic parameters from isothermal and/or multiple constant heating rate temperature programmes. Isoconversional or model-free approaches are often implemented for the determination of process activation energies as no prior knowledge of the particular reaction model is required. A most important use of isoconversional methods is that they can account for the complexities of solid-state processes as most are characterized by a changing rate-determining step as a function of temperature or time. Modellistic approaches are more restrictive as they confer an assumed reaction mechanism with constant Arrhenius parameters over a particular range of reaction extents (α). Their use in combination with isoconversional methods does, however, provide insight as to the type of reaction mechanism and process energetics [1].

A number of studies reported on the accuracies of integral (approximation based and without) and differential isoconversional methods for activation energy (E) determination. These include reports from Gao et al. [2] on the accuracies of the approximation-based integral methods of Ozawa and Kissinger–Akahira–Sunose. Starink [3], Šimon [4] and Sbirrazzuoli et al. [5] expanded accuracy evaluations to both integral and differential isoconversional methods. For integral isoconversional methods, it is generally accepted that a non-approximation-based direct numerical integration of experimental data over small

Electronic supplementary material The online version of this article (doi:10.1007/s10973-016-5244-x) contains supplementary material, which is available to authorized users.

✉ D. Grooff
dgrooff@nmmu.ac.za

[1] Department of Chemistry, Nelson Mandela Metropolitan University, Port Elizabeth 6031, South Africa

[2] Center of Excellence for Pharmaceutical Sciences, Faculty of Health Sciences, North-West University, Potchefstroom Campus, Potchefstroom 2520, South Africa

reaction intervals (advanced isoconversional method) [6] are superior to approximation-based methods and most representative of the 'actual' E at that specific stage of reaction. Šimon [4] as well as Sbirrazzuoli et al. [5] concluded that accurate methods for 'actual' E determination are based on direct experimental data such as instantaneous reaction rates for differential Friedman [7] or Advanced isoconversional method. These conclusions, however, are derived from theoretical principles [4], simulated and experimental DSC data [5]. Criado et al. [8] investigated the ability of the isoconversional methods of Ozawa and Friedman to account for the variation in 'actual' E with temperature during non-isothermal heating. They reported that E values from Friedman, contrary to Ozawa method, exhibited close agreement with E values from a simulated first-order process with varying E versus α dependence. Both methods, however, yielded apparent Es (with dependence on range of heating rates used) when applied to simulated competitive (overlapping) reactions. The Friedman method has therefore limitations in terms of the accurate evaluation of simultaneous processes. Starink [3] and Sbirrazzuoli [5] reported that the accuracy of Friedman is also related to errors in the estimation of instantaneous reaction rates and that approximated integral methods could prove more reliable. It would therefore be of interest to investigate whether similar conclusions could be drawn from experimental data in particular TG analysis where the above-mentioned integral and differential methods are widely reported in the scientific literature. TG analysis typically generates data in integral [reaction extent (α) vs. time (t) or temperature (T)] format. The use of differential isoconversional methods requires data conversion to differential format ($\mathrm{d}\alpha/\mathrm{d}t$ vs. t or T) which may be associated with increased baseline noise. This often necessitates the application of curve smoothing procedures which may ultimately influence the obtained E and subsequent kinetic parameters that stemmed from a differential approach.

This study investigated accuracies of integral, differential isoconversional (iso- and non-isothermal) and model fitting (isothermal) methods for the estimation of the 'actual' E from experimental TG data of the dehydration of a hydrate form of roxithromycin. Roxithromycin, an erythromycin derivative consisting of a 14-membered lactone ring, is used for the treatment of bacterial infections. Mallet et al. [9] have reported on its hydrate formation tendency via solvent exchange upon exposure of its acetonitrile solvate to humidity. The dehydration kinetic parameters are finally discussed in the context of the structural characterization of the mono- and anhydrate forms of roxithromycin.

Theory of kinetic methods used

The rate of a solid-state reaction can be represented by the following differential equation:

$$\frac{\mathrm{d}\alpha}{\mathrm{d}t} = A\exp(-E/RT)\cdot f(\alpha) \tag{1}$$

where the conversion rate ($\mathrm{d}\alpha/\mathrm{d}t$) at temperature ($T$) can be related to the Arrhenius parameters [E and pre-exponential factor (A)] and reaction model ($f(\alpha)$). For non-isothermal studies, $\mathrm{d}\alpha/\mathrm{d}t = (\mathrm{d}\alpha/\mathrm{d}T)*\beta$ with $\mathrm{d}\alpha/\mathrm{d}T$ and β represent the non-isothermal reaction rate and heating rate, respectively.

Isothermal

Equation 1 can be converted to its isoconversional form to give the Friedman equation [7]:

$$\ln\left(\frac{\mathrm{d}\alpha}{\mathrm{d}t}\right)_{\alpha,\mathrm{i}} = \ln[f(\alpha)A_\alpha] - \frac{E_\alpha}{RT_{\alpha,\mathrm{i}}} \tag{2}$$

E_α (activation energy at α) was calculated from the slopes of the plots of $\ln(\mathrm{d}\alpha/\mathrm{d}t)_{\alpha,\mathrm{i}}$ against $1/T_\mathrm{i}$. T_i represents the ith isothermal temperature. The integral form of the reaction model ($g(\alpha)$) obtained on integration of Eq. (1) according to:

$$g(\alpha) = A\int_0^t \exp(-E/RT)\cdot \mathrm{d}t = A\exp(-E/RT)\cdot t = k.t \tag{3}$$

was converted to the standard integral isoconversional form:

$$\ln t_{\alpha,\mathrm{i}} = \ln\left[\frac{g(\alpha)}{A_\alpha}\right] + \frac{E_\alpha}{RT_\mathrm{i}} \tag{4}$$

where E_α was calculated from the slopes of the plots of $\ln t_{\alpha,\mathrm{i}}$ against $1/T_\mathrm{i}$. $t_{\alpha,\mathrm{i}}$ represents the time to reach α at T_i.

Non-isothermal

For the non-isothermal form of the Friedman equation, the non-isothermal conversion rate $(\mathrm{d}\alpha/\mathrm{d}T)_{\alpha,\mathrm{i}}$ at α for the ith heating rate β_i was incorporated:

$$\ln\left[\beta_\mathrm{i}\left(\frac{\mathrm{d}\alpha}{\mathrm{d}T}\right)_{\alpha,\mathrm{i}}\right] = \ln[f(\alpha)A_\alpha] - \frac{E_\alpha}{RT_{\alpha,\mathrm{i}}} \tag{5}$$

and evaluated the same way as Eq. (2). The integral form of Eq. (1):

$$g(\alpha) = \frac{A}{\beta}\int_0^T \exp\left(\frac{-E}{RT}\right)\mathrm{d}T = \frac{A}{\beta}I(E,T) \tag{6}$$

does not have an analytical solution but many approximations. It can generally be represented by:

$$g(\alpha) = \left(\frac{AE}{\beta R}\right)\cdot p(x) \tag{7}$$

where $x = E/RT$ and $p(x)$ the approximation. The Kissinger–Akahira–Sunose method (KAS) [10, 11] can be derived from an approximated form of $p(x)$:

$$p(x) \cong \exp(-x)/x^2 \tag{8}$$

which solves to Eq. (9):

$$\ln\left(\frac{\beta_\mathrm{i}}{T^2}\right) = \mathrm{cons\,tan}\,t - \frac{E_\alpha}{RT_{\alpha,\mathrm{i}}} \tag{9}$$

The equation is generally considered reliable from $20 \le x \le 50$. E_α can be evaluated from the plot of $\ln(\beta_i/T^2)$ versus $1/T_{\alpha,\mathrm{i}}$. The slightly modified form (KAS-MOD) from Starink [3] (considered more accurate):

$$\ln\left(\frac{\beta_\mathrm{i}}{T_{\alpha,\mathrm{i}}^{1.92}}\right) = \mathrm{Const} - 1.0008\left(\frac{E_\alpha}{RT_\alpha}\right) \tag{10}$$

was used for E_α determination. The rational approach by Senum and Yang [12] has been proposed as accurate for the fourth-degree approximation (SY) [3, 13]:

$$p(x) = \frac{\exp(-x)\ \mathrm{x}^3 + 18\mathrm{x}^2 + 86\mathrm{x} + 96}{x\ \ x^4 + 20x^3 + 120x^2 + 240x + 120} \tag{11}$$

This approximation, incorporated into the expression for the temperature integral:

$$I(E,T) = \left(\frac{E}{R}\right)p(x) \tag{12}$$

was used to calculate E_α, from minimization of the following function [14]:

$$\sum_{i=1}^{n}\sum_{j\neq i}^{n}\frac{[I(E_\alpha, T_{\alpha,\mathrm{i}})\beta_\mathrm{j}]}{[I(E_\alpha, T_{\alpha,\mathrm{j}})\beta_\mathrm{i}]} = \min \tag{13}$$

The most accurate integral approach [6] involves the numerical integration [advanced nonlinear method (ADV-NN)] of the experimental data over short time intervals according to:

$$J[E_\alpha, T(t_\alpha)] = \int_{t_{\alpha-\Delta\alpha}}^{t_\alpha} \exp\left[\frac{-E_\alpha}{RT(t)}\right]\mathrm{d}t \tag{14}$$

The J integral (Eq. 14) was evaluated with the trapezoid rule with α varied from $0.02 - \Delta\alpha$ to $0.90 - \Delta\alpha$ with $\Delta\alpha = 0.02 = (m)^{-1}$. This gave m (the number of equidistant values of α) = 50. The calculated J integrals were minimized according to Eq. (15):

$$\sum_{i=1}^{n}\sum_{j\neq i}^{n}\frac{[J(E_\alpha, T_\mathrm{i}(t_\alpha)]}{[J(E_\alpha, T_\mathrm{j}(t_\alpha)]} = \min \tag{15}$$

Experimental

Materials

Roxithromycin [assay ≥90 % (HPLC)] was purchased from Sigma-Aldrich and used without further purification for all kinetic studies.

Methods

Simultaneous DSC-TG and DSC

Simultaneous differential scanning calorimetry and thermogravimetric analysis (DSC-TG) were performed on a SDT Q600 (from TA Instruments, Johannesburg, South Africa) using a controlled temperature programme. A complete calibration was performed prior to the characterization and kinetic studies. This included TG mass (calibration masses provided by TA Instruments), temperature (performed with high-purity indium and zinc metal), heat flow (sapphire standard) and cell-constant calibrations (zinc). All studies were performed under dry nitrogen purge at a flow rate of 100 mL min^{-1}. This flow rate was deemed sufficient for the effective removal of water vapour (from dehydration reaction) inside the furnace after various flow rates (10–150 mL min^{-1}) were tested. The dehydration and melting behaviour were characterized by dynamic heating experiments at 10 °C min^{-1} from 23 to 140 °C. A Q200 DSC (from TA Instruments, Johannesburg, South Africa), temperature calibrated with indium and zinc, was used as a heater to prepare an anhydrate form of roxithromycin (10 °C min^{-1} from ambient temperature to 110 °C). The prepared form was removed, weighed by placement inside a tarred ceramic sample pan (inside SDT Q600 furnace) and immediately reheated at 10 °C min^{-1} from 23 to 140 °C. In another experiment, prepared anhydrate crystals were structurally analysed with single-crystal X-ray diffraction (SC-XRD) (section: Dehydration mechanism and structural characterization).

Hot-stage microscopy (HSM)

A Nikon Eclipse E400 microscope (Nikon Instruments, Tokyo, Japan) equipped with camera and a Metratherm 1200d heater were used to visually monitor the thermally

stimulated dehydration of roxithromycin crystals. Captured images were analysed with NIS-Elements D32 software (Nikon Instruments, Tokyo, Japan).

Karl Fischer analysis

A Metrohm 870 KF Titrino Plus, connected to an 803 Ti stand, hosting the titration vessel (Herisau, Switzerland) was used to calculate the moisture content of the roxithromycin. It was calibrated using a predetermined mass of water (25–30 μL) and a Hydranal® water standard 10.0 [1 g contains 10.0 mg water (1 %)]. Approximately 100 mg of sample was used for moisture determination. Analyses were performed in triplicate.

X-ray diffraction

X-ray diffraction studies were performed at 200 K using a Bruker Kappa Apex II diffractometer with graphite monochromated Mo–Kα radiation ($\lambda = 0.71073$ Å). APEXII [15] was used for data collection and SAINT [15] for cell refinement and data reduction. The structure was solved by direct methods using SHELXS-2014 [16] and refined by least-squares procedures using SHELXL-2014 [16] with SHELXLE [17] as a graphical interface. Data were corrected for absorption effects using the numerical method implemented in SADABS [15]. Reflections obstructed by the beam-stop were omitted from the refinements. All non-hydrogen atoms were refined anisotropically. The carbon-bound H atoms were placed in idealized geometrical positions and allowed to ride on their parent atoms in the refinement cycles. The H atoms of the methyl groups and hydroxyl groups were allowed to rotate to best fit the experimental electron density (HFIX 137 and HFIX 147, respectively, in the SHELX program suite [16]). The water-bound hydrogens were located in a Fourier map and restrained (O–H = 0.84 and H···H = 1.34 Å).

Supplementary data for the monohydrate (CCDC 1411181) and dehydrated sample (CCDC 1411213) are available from the CCDC, 12 Union Road, Cambridge CB2 1EZ, UK, on request. These data can be obtained free of charge from the Cambridge Crystallographic Data Centre via http://www.ccck.cam.ac.uk/data_request/cif.

Kinetic studies and data treatment

All calculations involving data treatment, curve fitting and kinetic analysis were performed with Excel software (MS Office 2010) (Microsoft Corporation, Redmond, USA). Regression statistics was performed in Excel with 95 % confidence limits. A previous report [18] on the influence of particle size and sample mass on the reaction kinetics of thermally stimulated processes was considered. It was decided to use samples for dehydration studies as is (from supplier), as the achievement of particle size uniformity from a mechanical sieving process could be negated by the possible formation of reactive sites. Sample mass was kept constant at 3 (±0.2) mg, so as to minimize experimental deviations attributed to temperature gradients and trapped waters of hydration. The extent of the thermally stimulated dehydration reaction was monitored with the TG segment of the SDT Q600. The temperature-controlled heating regimes included both isothermal and non-isothermal studies for kinetic investigations.

Isothermal studies were conducted in duplicate at temperatures of 40, 47, 50, 55 and 60 °C for a period of 3 h. This was followed by a temperature ramp of 10 °C min^{-1} to 140 °C. The temperature ramp was required as isothermal temperatures up to 47 °C yielded incomplete dehydration (40 °C and 47 °C at 86 and 95 % dehydration, respectively) for the 3-h segment. In an attempt to minimize the unavoidable initial non-isothermal stage of the isothermal heating programme (and consequent effect on the conversion rate), a three-step approach was adopted for the isothermal experiments. The first step involved zeroing of the ceramic sample and reference pan mass (tarring inside furnace chamber of SDT Q600), sample pan removal followed by the introduction of a pre-weighed (in Mettler Toledo (Columbus, USA) microbalance) quantity of roxithromycin inside the sample pan. This ensured better sample size control relative to the exclusive use of only the instrument weighing mechanism. The second step involved furnace conditioning to the temperature of the isothermal study by heating to the isothermal temperature, followed by a 7-min equilibration time. The sample pan (with weighed sample) was then quickly reintroduced in the third step after the isothermal study commenced. The introduction of the sample (from ambient temperature) to the hotter furnace temperature did imply an initial equilibration period as the sample temperature adjusted to the isothermal condition. This equilibration period was, however, viewed as less intrusive relative to the problem of ensuing mass loss (from dehydration) if sample was kept in furnace during the furnace preparation process (step 2).

The curve of absolute mass (m) versus time (t) at isothermal temperature (T_i) was analysed with Universal Analysis 2000 software from TA Instruments and converted to numerical format in Excel. The numerical data points (numbered more than 3600 per isothermal temperature) were used for computation of the dehydration extent (α) according to:

$$\alpha = \frac{m_0 - m_t}{m_0 - m_\infty} \tag{16}$$

The masses m_0, m_t and m_∞ represented the initial mass, mass after reaction time (t) and the final mass after

completion of the dehydration reaction, respectively. The numerical format of the derivative thermogravimetric (DTG) signal in mass loss time^{-1} was converted to the fractional loss rate (dα/dt) according to:

$$\frac{d\alpha}{dt} = \text{mass loss} \cdot \text{time}^{-1} / (m_0 - m_\infty) \quad (17)$$

The DTG signal is known for its sensitivity and frequently produces noisy data for TG experiments. This presented a source of interference on calculation of dα/dt from Eq. (17) (Fig. 1). In an attempt to minimize the interference of baseline noise on kinetic computations, polynomial curve fitting (using linest) was performed on α versus t data (calculated from Eq. 16). The coefficient of determination (r^2) ranged from 0.9945 to 0.9995 for all fits. α versus t curves were recalculated from the polynomial functions and converted to dα/dt by numerical differentiation.

Non-isothermal studies were conducted in duplicate at heating rates (β_i) of 1, 1.5, 2, 5, 7 and 10 °C min^{-1}. Samples were equilibrated at 23 °C for 5 min followed by heating at a set heating rate to 140 °C. The heating rate, i, was calculated from the slope of the temperature versus time plot in Universal Analysis. The non-isothermal TG data were treated analogously to data from isothermal studies. That is conversion of m versus $T(K)$ and corresponding t data at heating rate (β_i) to numerical format (from ~1300 to 2500 data points) using Excel. α was calculated with Eq. 16 with m_t now representing the mass remaining at furnace temp (T). The non-isothermal reaction rate (dα/dT) was calculated from the DTG signal (mass loss K^{-1}) according to:

$$\frac{d\alpha}{dT} = \text{mass loss} \cdot K^{-1} / (m_0 - m_\infty) \quad (18)$$

The dα/dT curve (Fig. 2) exhibited some irregularities (especially at low α) due to the sensitivity of the DTG signal to heating rate and baseline fluctuations in TG signal. The experimental data were subjected to polynomial curve fits (linest, $r^2 > 0.9991$) in order to represent the data in terms of equidistant α values (required for ADV-NN) with the corresponding values of T and t. The interpolations were performed according to $T = f(\alpha)$ and $t = f(\alpha)$. Numerical differentiation of the reconstructed $\alpha - T$ data yielded the smoothed dα/dT curve.

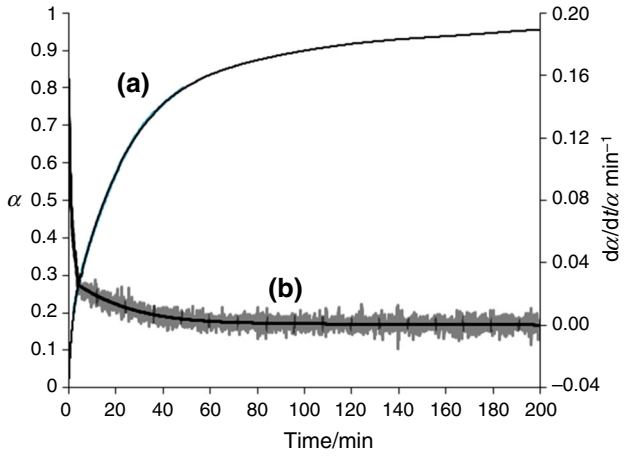

Fig. 1 Alpha (α) and conversion rate (dα/dt) versus time curves (at 46.05 °C) to illustrate typical baseline noise associated with DTG signal for isothermal dehydrations (performed from 39.09 to 59.09 °C) of roxithromycin monohydrate. Curves *a*, *b* (depicted in *grey*) represent α (Eq. 16) and dα/dt (Eq. 17) values calculated from experimental mass data and the DTG signal, respectively. The *solid line* fit to dα/dt was derived from polynomial curve fitting to α versus time data and numerical differentiation of data derived from the polynomial function

Results and discussion

Thermal characterization

Analysis of the DSC-TG curves (Fig. 3) of roxithromycin (obtained at 10 °C min^{-1}) showed a mass loss of 2.1 % from ambient up to ~110 °C. The downward direction of the corresponding heat flow signal suggested that the mass loss was endothermic. The endothermic event with onset temperature at 116.3 °C (T_{mp}, Fig. 3) corresponded with other reported literature melting onsets of 114.5 °C [9] and 116.2 °C [19], respectively. Karl Fischer analysis, performed in triplicate [2.34 % (±0.06 %)], confirmed that the initial loss can be attributed to coordinated water. The experimental water determinations were similar to the theoretical prediction of 2.1 % for a monohydrate form. In a separate experiment, roxithromycin was heated at

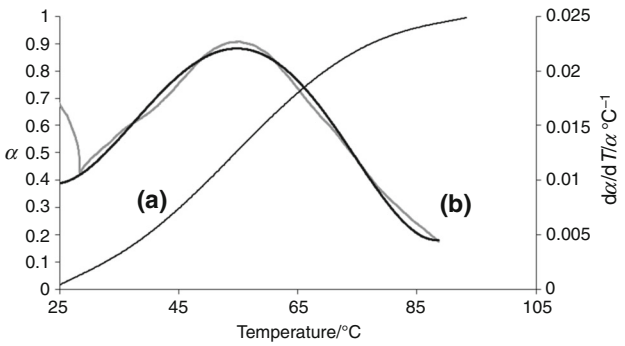

Fig. 2 Alpha (α) and conversion rate (dα/dT) versus temperature (°C) curves (illustrated for heat rate 1.50 °C min^{-1}), to show typical discontinuities associated with the DTG signal for non-isothermal (1–10 °C min^{-1}) dehydrations of roxithromycin monohydrate. Curves (*a*) and (*b*) (depicted in *grey colour*) represent α (Eq. 16) and dα/dT (Eq. 18) values calculated from experimental mass data and the DTG signal. The *solid line* fit to dα/dT was derived from numerical differentiation of data from polynomial curve fit (α vs. T)

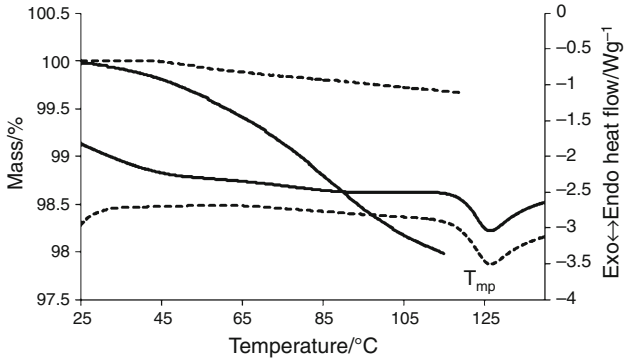

Fig. 3 DSC and TG data at 10.01 °C min^{-1} to illustrate the thermal behaviour of the monohydrate (*solid lines*) and anhydrate forms (*dashed lines*) of roxithromycin

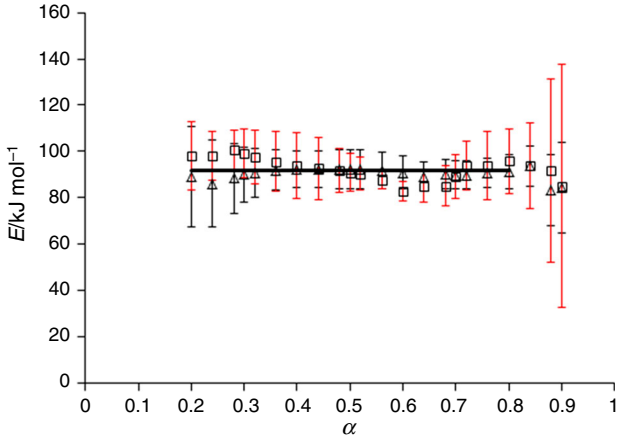

Fig. 4 Activation energy (E, kJ mol^{-1}) computed as a function of α for isothermal studies from isoconversional integral [*triangle*, ±SDs (*black vertical bars*)] and Friedman [*square*, ±SDs (*red vertical bars*)] methods. The *solid line* represents E from model fitting (α range 0.2–0.8). (Color figure online)

10 °C min^{-1} to 110 °C in the Q200 DSC, after which the sample was removed, reweighed and reheated in the DSC-TG at 10 °C min^{-1} from 23 to 140 °C. The TG curve of the reheated roxithromycin showed a gradual loss of ~0.4 % up to 120 °C which suggested that roxithromycin was converted to the anhydrate form. The corresponding DSC curve only showed the melting endotherm at ~116 °C which confirmed that the anhydrate form was crystalline. It can be concluded that roxithromycin existed as a monohydrate and that the thermally stimulated dehydration was not accompanied by a destruction of the crystal structure. For structural characterization, refer to section: Dehydration mechanism and structural characterization.

E results, computed from integral and differential data

E from isothermal studies

Integral data are expected to be more reliable for E determination due to the higher signal-to-noise ratio relative to differential data. E values obtained from standard integral isoconversional method are therefore expected to provide a benchmark to which E results from the differential Friedman approach should conform. Figure 4 illustrates E values (α range 0.20–0.90) for isothermal (39.08–59.09 °C) studies calculated from standard integral, Friedman and model fitting (α range 0.20–0.80) methods. The chosen α from ≥0.20 was assumed to be more representative of coordinated water from the crystal structure as well as less interference from the initial non-isothermal condition on the kinetic analysis (for isothermal studies). The general horizontal trend of calculated E values from $\alpha = 0.20 - 0.80$ suggested that a single rate-determining dehydration step applied over the isothermal temperature range. In the above-mentioned α range, E values (±SD in brackets) calculated from standard integral isoconversional method yielded a greater consistency for E from 86.1 (±18.7) to 92.4 (±8.0) kJ mol^{-1} with average at 90.6 (average SD ± 9.5) kJ mol^{-1}. E values calculated from the differential Friedman were not significantly different [averaged at 92.7 (average SD ± 10.2) kJ mol^{-1}] but with greater scatter as E values varied from 82.8 (±4.1) to 100.5 (±8.7) kJ mol^{-1}. This suggested that the differential data (derived from numerical differentiation of α vs. t polynomial fits) included a larger associated random error in the E estimates. The relative constancy in E was further investigated by fitting nine (deceleratory) solid-state reaction models (Table 1) according to Eq. (3) (and calculating E from Arrhenius's plots using obtained k values) over α range 0.20–0.80 to all isothermal data (39.08–59.09 °C). The E results (Table 2) were fairly independent of the chosen reaction model [ranged from 90.4 (±6.9) to 91.8 (±7.0) kJ mol^{-1}] and very similar to the isoconversional predicted values. The model of best statistical fit ($D3$, discussed in section on Dehydration mechanism…) gave E at 91.6 (±6.9) kJ mol^{-1}, intermediate between the standard integral and Friedman predictions. Findings by Sánchez-Jiménez et al. [20] were furthermore considered relevant to this study in that Arrhenius parameters from model fitting, applicable to single solid-step reaction, can be considered reliable irrespective of the kinetic model used.

E from non-isothermal studies

E from non-isothermal studies (Fig. 5) exhibited a general decrease as a function of α for all integral (KAS-MOD, SY, ADV-NN) as well as the differential Friedman method. This indicated a change in the rate-determining dehydration step which could be due to a changing dehydration mechanism with temperature increase. This is plausible as the non-isothermal kinetic studies covered a wider furnace temperature range (relative to the 20 °C range for

Table 1 Differential ($f(\alpha)$) and integral forms ($g(\alpha)$) of deceleratory solid-state reaction models

Model	$f(\alpha)$	$g(\alpha)$
1. Contracting area (R2)	$2(1-\alpha)^{1/2}$	$1-(1-\alpha)^{1/2}$
2. Contracting volume (R3)	$3(1-\alpha)^{2/3}$	$1-(1-\alpha)^{1/3}$
3. 1-D diffusion (D1)	$1/(2\alpha)$	α^2
4. 2-D diffusion (D2)	$-[1/\ln(1-\alpha)]$	$((1-\alpha)\ln(1-\alpha))+\alpha$
5. 3-D diffusion–Jander (D3)	$[3(1-\alpha)^{2/3}]/2(1-(1-\alpha)^{1/3})]$	$(1-(1-\alpha)^{1/3})^2$
6. Ginstling–Brounshtein (D4)	$3/[2((1-\alpha)^{-1/3}-1)]$	$1-(2/3)\alpha-(1-\alpha)^{2/3}$
7. First order (F1)	$(1-\alpha)$	$-\ln(1-\alpha)$
8. Second order (F2)	$(1-\alpha)^2$	$[1/(1-\alpha)]-1$
9. Third order (F3)	$(1-\alpha)^3$	$(1/2)[(1-\alpha)^{-2}-1]$

Table 2 Arrhenius parameters [activation energy (E) and pre-exponential factor ($\ln(A)$)] with ±SD (in brackets) for the isothermal dehydration (39.09–59.09 °C) of roxithromycin monohydrate after fitting (α range 0.20–0.80) to deceleratory solid-state reaction models

Model	r^2	E/kJ mol^{-1}	$\ln(A)$/min^{-1}
R2	0.9604	91.1 (±6.8)	29.5 (±2.5)
R3	0.9707	91.2 (±6.8)	29.3 (±2.5)
D1	0.9738	91.3 (±6.9)	29.9 (±2.6)
D2	0.9893	91.5 (±6.9)	29.8 (±2.6)
D3	0.9960	91.6 (±6.9)	28.8 (±2.6)
D4	0.9931	91.5 (±6.9)	28.4 (±2.6)
F1	0.9862	91.3 (±6.8)	30.8 (±2.5)
F2	0.9926	91.7 (±6.8)	31.9 (±2.5)
F3	0.9492	91.8 (±7.0)	33.1 (±2.6)

The coefficient of determination (r^2), represents the averaged fit from all isothermal temperatures (according to $g(\alpha)=kt$)

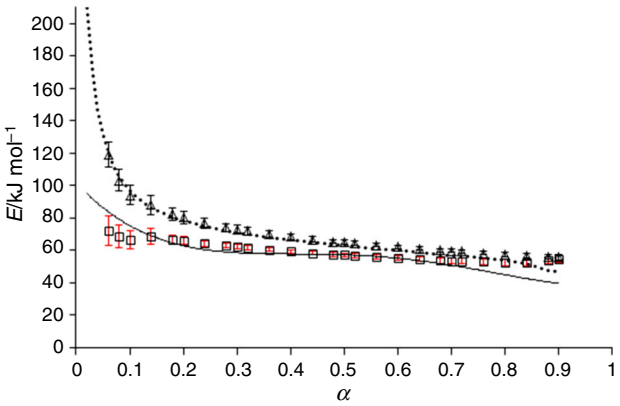

Fig. 5 Activation energy (E, kJ mol^{-1}) as a function of α for non-isothermal studies calculated from Friedman (*square*), KAS-MOD (*triangle*), SY (*dotted line*) and ADV-NN (*solid line*) isoconversional methods (±SDs indicated for Friedman and KAS-MOD)

isothermal) from 23 to 120 °C. Sbirrazzuoli et al. [5], who evaluated the use of integral, differential and advanced isoconversional methods on systems that exhibit complex reaction mechanisms, concluded that the ADV-NN method [6] was the most accurate for E determinations. It was therefore assumed that E results (Fig. 5) calculated from ADV-NN procedure were most representative of the actual values. The E against α trend from ADV-NN method exhibited notable decreases in the initial (from zero up to α 0.2) and latter stages ($\alpha > 0.6$) of the dehydration process. A relative constancy in the central α range between α 0.2 and 0.6 (where E gradually decreased from 64.4 to 58.2 kJ mol^{-1}) pointed to a similar rate-determining step. The Friedman method which utilizes instantaneous non-isothermal reaction rates for E calculations yielded very similar results (relative to ADV-NN) with an average % relative error of 2.0 % from α 0.14 (2.8 %) to 0.70 (2.7 %). The deviations in E (below and above $\alpha = 0.14$ and 0.70, respectively) was interpreted in terms of the slower instantaneous reaction rates at the beginning and latter stages of dehydration where the resulting error in rate estimation will be greatest.

E values calculated from the approximation-based integral methods of KAS-MOD and SY were very similar (up to $\alpha = 0.70$) but deviated more (relative to Friedman) from the ADV-NN method. Over the same α range, the % relative errors for KAS-MOD (average % relative error 18.8 %) were 24.9 and 14.5 % at α 0.14 and 0.70, respectively. The method of SY was similar (average % relative error 15.5 %) at 22.3 and 9.3 % for α 0.14 and 0.70, respectively.

From $\alpha > 0.70$, E values from KAS-MOD deviated from SY following the downward trend of E values from ADV-NN method. The closer correspondence of the differential Friedman method (relative to integral methods

that employ approximations to the temperature integral) to E results from ADV-NN suggested that the application of the differential Friedman equation to experimental TG data seemed more accurate than the use of approximated integral isoconversional methods.

Dehydration mechanism and structural characterization

The distinctive shape of α and $d\alpha/dt$ versus t curves (Fig. 1) for isothermal data indicated that dehydration was deceleratory. The most suitable kinetic models for this type of dependence include diffusion (D)-, order (F)- and geometrical contraction (R)-based models [21]. The results of curve fitting (α-range 0.2–0.8) deceleratory-type solid-state reaction models (Table 1) to experimental data from all isothermal temperatures (according to $g(\alpha) = kt$) are represented in Table 2 where the coefficient of variation (r^2) represented the averaged value from fits at all isothermal temperatures for each model. The fitting procedure did not clearly favour a particular reaction model as indicated by the best fits (but not significantly different) for $D3$ (r^2 0.9962), $D4$ (r^2 0.9931) and $F2$ (r^2 0.9926). The suitability of a particular deceleratory model to experimental dehydration data was further investigated with master plots [22] based on the generalized time concept (θ), as defined by Eq. (19):

$$\theta = \int_0^t \exp(-E/RT)\mathrm{d}t \tag{19}$$

θ represents the time to reach a particular α at infinite temperature. The derivative of Eq. (19):

$$\frac{\mathrm{d}\theta}{\mathrm{d}t} = \exp(-E/RT) \tag{20}$$

on substitution into Eq. (1) can be rearranged to give the expression for generalized reaction rate:

$$\frac{\mathrm{d}\alpha}{\mathrm{d}\theta} = Af(\alpha) \tag{21}$$

With $\alpha = 0.5$ as reference, the reduced-generalized reaction rate can be derived from Eq. (21):

$$\frac{\mathrm{d}\alpha/\mathrm{d}\theta}{(\mathrm{d}\alpha/\mathrm{d}\theta)_{0.5}} = \frac{f(\alpha)}{f(0.5)} \tag{22}$$

The theoretical master plots (computed from Eq. 22 and plotted as $f(\alpha)/f(0.5)$ against α) of the F and D models are represented by the line curves in Fig. 6a, b. The isothermal experimental rate ($d\alpha/dt$) data over α range 0.2–0.8 [where E was considered constant (Fig. 4)] were expressed in terms of the reduced-generalized reaction rate according to Eq. (23):

$$\frac{\mathrm{d}\alpha/\mathrm{d}\theta}{(\mathrm{d}\alpha/\mathrm{d}\theta)_{0.5}} = \frac{\mathrm{d}\alpha/\mathrm{d}t}{(\mathrm{d}\alpha/\mathrm{d}t)_{0.5}} \tag{23}$$

and plotted in Fig. 6a. The experimental isothermal data clearly obeyed different reaction models over different α ranges. At the lower isothermal temperatures of 39.09 and 46.05 °C, the dehydration reaction mechanism was intermediate between $F1$ and $D1$ in α range 0.2–0.3, $D1$ in α range 0.36–0.40 crossing to eventual multidimensional diffusion ($D2$, $D4$ and $D3$) from α 0.5 to 0.8. The other isothermal temperatures (49.21–59.09 °C) exhibited clear D-based mechanisms of $D1$ (α 0.2–0.4) crossing to multidimensional $D2$ (α 0.44–0.64) and $D3$ (α 0.8).

The mechanistic aspects of the dehydration mechanism were also investigated for non-isothermal studies. Since master plots are only valid for conditions of constant E over conversion range (α), experimental data were only considered in the central conversion region [from α 0.3 to 0.6 (Fig. 5)] where a relatively constant E (from ADV-NN) was computed. The experimental rate ($d\alpha/dt$), central E value (from ADV-NN) and T data over this α range were used to calculate the reduced-generalized reaction rate according to Eq. (24):

$$\frac{\mathrm{d}\alpha/\mathrm{d}\theta}{(\mathrm{d}\alpha/\mathrm{d}\theta)_{0.5}} = \frac{\mathrm{d}\alpha/\mathrm{d}t}{(\mathrm{d}\alpha/\mathrm{d}t)_{0.5}} \frac{\exp(E/RT)}{\exp(E/RT_{0.5})} \tag{24}$$

and plotted in Fig. 6b. The dehydration mechanism appeared very similar to isothermal studies in that a varying D model applied over this α range. The dehydration mechanism conformed to $D1$ up to α 0.35, crossing to $D2$ (from α 0.44) and higher-dimensional diffusion ($D4$, $D3$) up to α 0.6.

HSM analysis of the commercial monohydrate form revealed colourless irregular block-shaped crystals of varied diameters (30–175 μm in length) that remained morphologically intact upon heating to the anhydrate form. SC-XRD analysis (crystallographic data in Table 3) performed on the commercial roxithromycin monohydrate and the anhydrate form attempted to account for the observed thermally stimulated dehydration kinetics of commercial roxithromycin monohydrate. The results obtained for the monohydrate are in agreement with other workers [23, 24] in that the monohydrate form belonged to an orthorhombic crystal system with space group P212121.

Each asymmetric unit consists of one roxithromycin molecule and one water molecule, and there are four roxithromycin molecules in the unit cell. Figure 7 shows the unit cell packing viewed along the a-axis. A large number of potential hydrogen bonds (Fig. 8a) exist. Most of these are intramolecular, giving roxithromycin a rigid structure. The following intramolecular hydrogen bonds are noteworthy: O9–H9···O12, C16–H16···O4, C17–H17···O5,

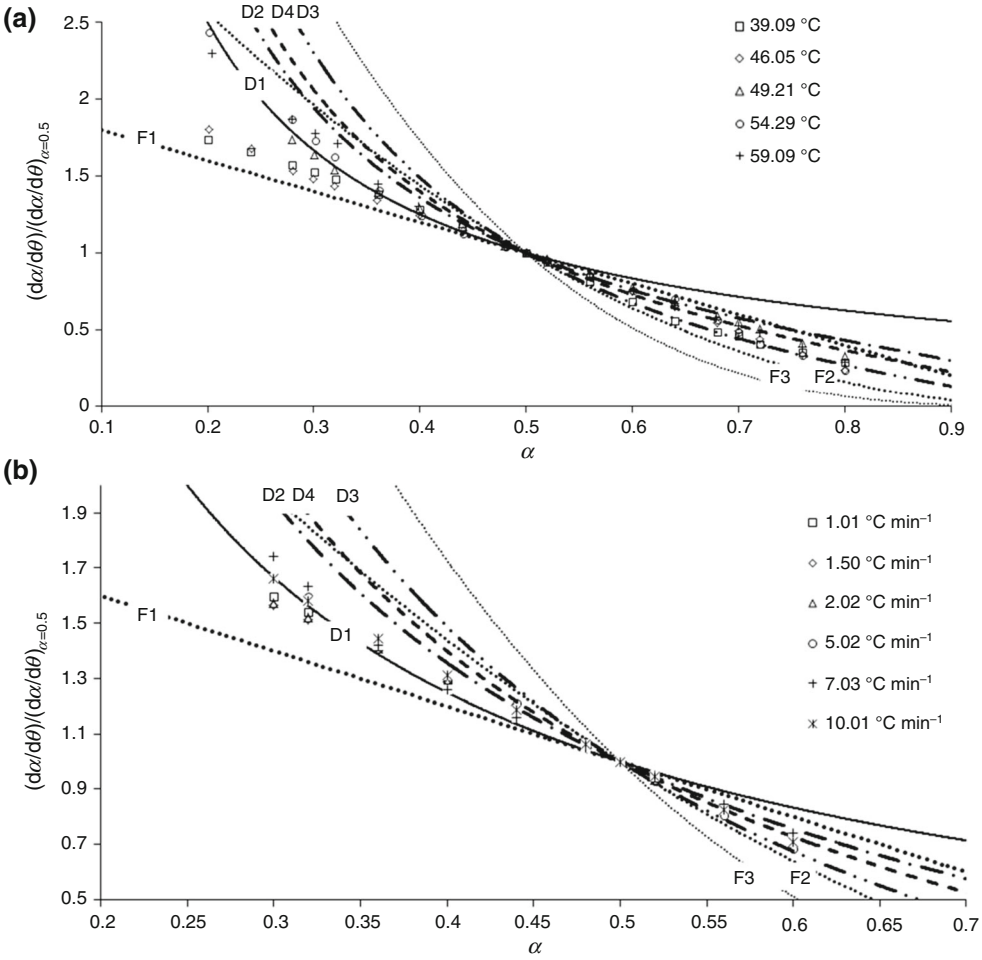

Fig. 6 A comparison of experimental masterplots of $(d\alpha/d\theta)/(d\alpha/d\theta)_{0.5}$ against α for **a** the isothermal dehydration (39.08, 46.05, 49.21, 59.09 °C) over α range 0.2–0.8 and **b** non-isothermal dehydration (1.01, 1.50, 2.02, 5.02, 7.03, 10.01 °C min^{-1}) over alpha range 0.3–0.6. The *line curves* represent the theoretical master plots

Table 3 Crystallographic and structure refinement data

	Monohydrate sample	Dehydrated sample
Empirical formula	$C_{41}H_{76}N_2O_{15}$, H_2O	$C_{41}H_{76}N_2O_{15}$, 0.25 (H_2O)
Formula weight	855.05	841.51
Crystal description	Colourless needle	Colourless block
Crystal system	Orthorhombic	Orthorhombic
Space group	P212121	P212121
a/Å	11.6581 (2)	11.4751 (5)
b/Å	16.8443 (4)	16.8598 (8)
c/Å	24.1092 (5)	24.3262 (11)
V/Å^3	4734.38 (17)	4706.3 (4)
Z	4	4
ρ_{calc}/g cm^{-3}	1.200	1.188
Total reflections	25,779	37,059
Unique reflections	11,026	11,701
R	0.0427	0.0329
*wR*2	0.0992	0.0837
Flack *x*	−0.3 (2)	−0.09 (14)

C25–H25C···O7 and C36–H36···O9. Each water molecule has three hydrogen bonds with a single roxithromycin molecule: O13–H13···O16, O16–H16A···O1 and O16–H16B···O11 with lengths of 1.95, 2.10 and 2.08 Å, respectively (Fig. 8a). The roxithromycin molecules are linked in an infinite change along the a-axis by the two hydrogen bonds O5–H5···N1^{i} and O8–H8···O5^{ii}.

SC-XRD analyses of the anhydrate indicated that dehydration occurred without any significant change to the crystal structure (Table 3). The dehydrated crystal tested still had a small amount of residual water left (approximately 25 mol %). Overlaying the roxithromycin molecules shows very little difference with a root-mean-square deviation (RMSD) of 0.0711 and a maximum position change of 0.259 Å for non-hydrogen atoms [25]. The only significant change in the structure is the rotation of the O13 hydroxy group (Fig. 8b) where the O13–H13···O16 hydrogen bond changes to O13–H13···N2 upon dehydration. With the water completely removed, the crystal structure shows a total void volume of 448.4 Å^3 (9.5 % of unit cell volume) calculated with a probe radius of 1.0 Å and grid spacing of 0.2 Å [25]. Figure 9 shows the voids. Although no clear channels are visible, the voids must be interlinked to allow the loss of water upon heating without change to the crystal structure. The thermally stimulated dehydration can therefore be interpreted in terms of an eventual multidimensional diffusional escape of water molecules via interlinked voids. The initial escape of bound water is likely to initiate close to surface and conform according to a diffusional loss of lower order ($D1$ and $D2$), whereas the later escape of inner water via void pathways created from prior escaped water molecules probably facilitated the change to higher-dimensional diffusion mechanism ($D3$ and $D4$). The influence of irregular particle shape and size distribution (from HSM analysis) could also have contributed to the observed multidiffusion models which may represent a deviation from the ideal or correct D model. Koga et al. [26] investigated the role of particle size distribution on kinetic parameters from solid-state reactions and concluded that an increase in particle size distribution contributed to deviations and the inability to discriminate the correct (or ideal) kinetic model within the same model class (example D). Widely different kinetic models (with different rate-determining steps) are, however, distinguishable even with large particle size distributions [26]. It is therefore possible that the observed D model changes with α (from master plots) be attributable to sample heterogeneities.

The relative constancy in E from isothermal studies is furthermore reconcilable with a constant H-bonding environment (3-H bonds per water to single roxithromycin molecule) for all coordinated water molecules in the hydrate structure. Non-isothermal studies reported a generalized decrease for E (as function of temperature and α) which can mostly be interpreted in terms of a weakening of

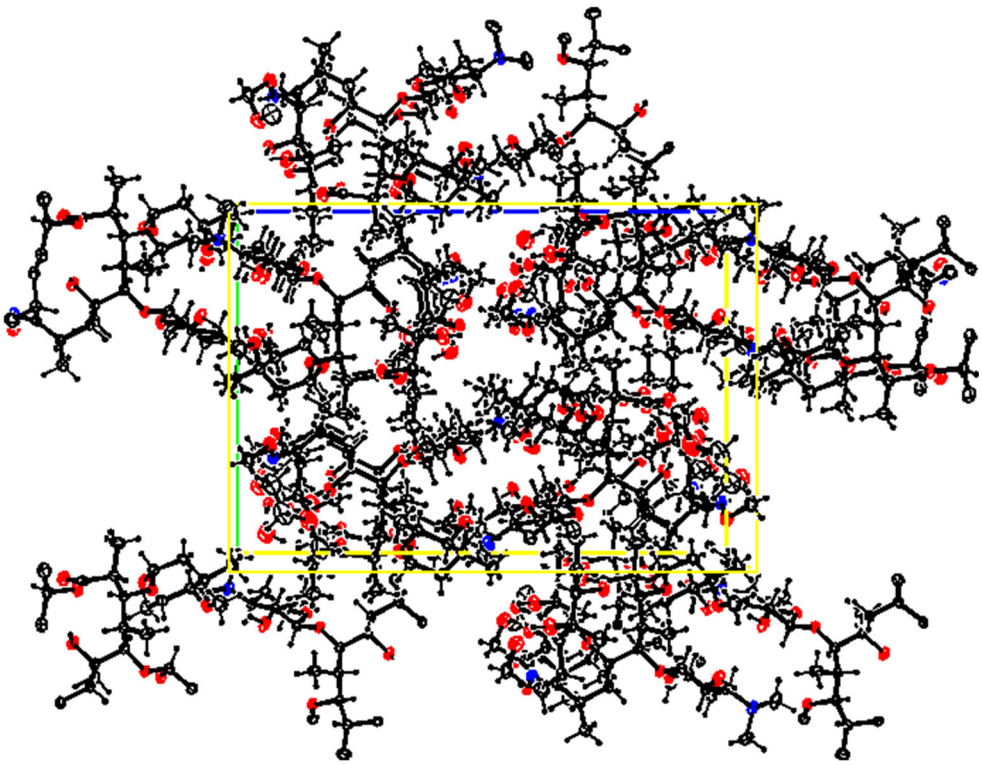

Fig. 7 Molecular packing of roxithromycin monohydrate, viewed along [1 0 0] (anisotropic displacement ellipsoids drawn at 50 % probability level)

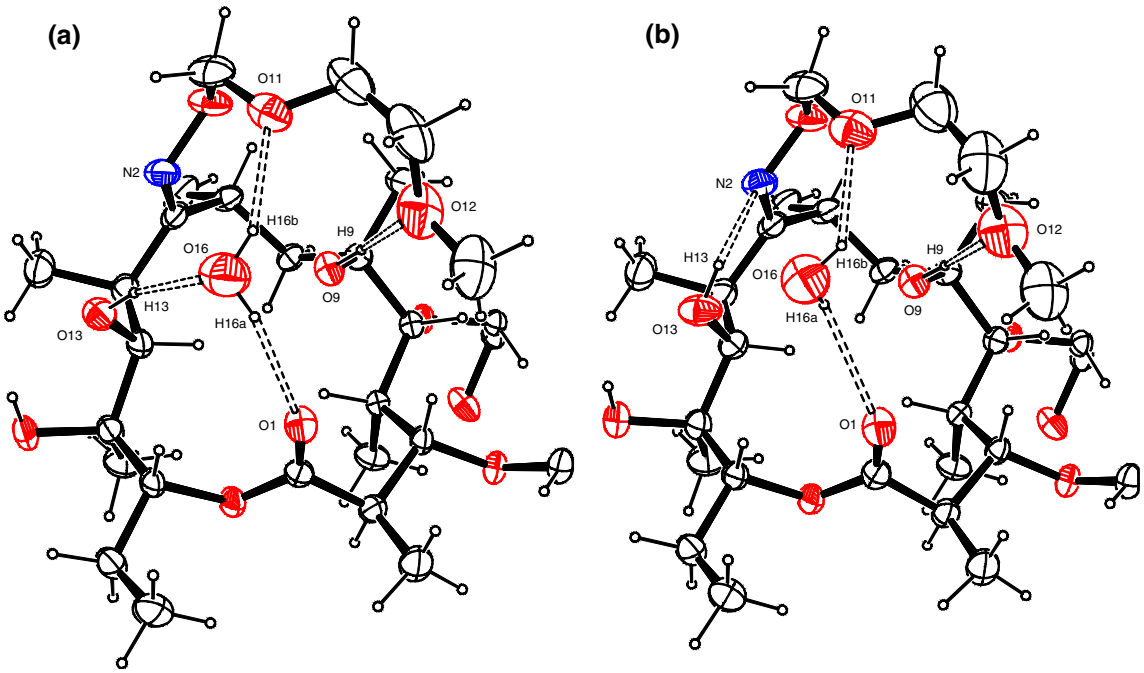

Fig. 8 Hydrogen bonding (*dashed bonds*) of the water molecule in **a** monohydrate sample and **b** partially dehydrated sample (anisotropic displacement ellipsoids drawn at 50 % probability level)

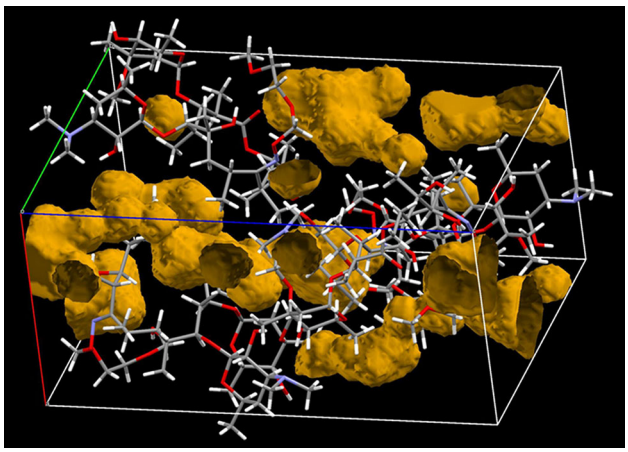

Fig. 9 Voids calculated with a probe radius of 1.0 Å and grid spacing of 0.2 Å

average H-bonding strength on increased temperature, probably brought about by increased lattice vibration and expansion effects.

Conclusions

The study concluded that E determination from the application of the differential Friedman isoconversional method to experimental TG data may approach similar accuracy to integral methods or may even prove superior to methods (non-isothermal) that rely on an approximation of the temperature integral. This greater correspondence of E results from Friedman method to ADV-NN method can be attributed to a significantly large differential signal where the error in the estimate of instantaneous reaction rate ($d\alpha/dT$) was less than the error introduced by the approximation of the temperature integral. The obtained kinetic parameters from model-free methods and generalized kinetic master plots were complementary to results from the structural characterization of the monohydrate and anhydrate forms of roxithromycin.

Acknowledgements The authors acknowledge the Nelson Mandela Metropolitan University (NMMU) and National Research Foundation (NRF) for research funding.

References

1. Khawam A, Flanagan DR. Complementary use of model-free and modelistic methods in the analysis of solid-state kinetics. J Phys Chem B. 2005;109:10073–80.
2. Gao Z, Nakada M, Amasaki I. A consideration of errors and accuracy in the isoconversional methods. Thermochim Acta. 2001;369:137–42.
3. Starink MJ. The determination of activation energy from linear heating rate experiments: a comparison of the accuracy of isoconversion methods. Thermochim Acta. 2003;404:163–76.
4. Šimon P. Isoconversional methods fundamentals, meaning and application. J Therm Anal Calorim. 2004;76:123–32.

5. Sbirrazzuoli N, Vincent L, Mija A, Guigo N. Integral, differential and advanced isoconversional methods complex mechanisms and isothermal predicted conversion-time curves. Chemom Intel Lab Syst. 2009;96:219–26.
6. Vyazovkin S. Modification of the integral isoconversional method to account for variation in the activation energy. J Comput Chem. 2001;22:178–83.
7. Friedman HL. Kinetics of thermal degradation of char-forming plastics from thermogravimetry. Application to a phenolic plastic. J Polym Sci C. 1964;6:183–95.
8. Criado JM, Sánchez-Jiménez PE, Pérez-Maqueda LA. Critical study of the isoconversional methods of kinetic analysis. J Therm Anal Calorim. 2008;92:199–203.
9. Mallet F, Petit S, Lafont S, Billot P, Lemarchand D, Coquerel G. Solvent exchanges among molecular compounds. Two extreme cases of pharmaceutical interest. J Therm Anal Calorim. 2003;73:459–71.
10. Kissinger HE. Reaction kinetics in differential thermal analysis. Anal Chem. 1957;29:1702–6.
11. Akahira T, Sunose T. Method of determining activation deterioration constant of electrical insulating materials. Res Rep Chiba Inst Technol. 1971;16:22–31.
12. Senum GI, Yang RT. Rational approximation of the integral of the Arrhenius function. J Therm Anal. 1977;11:445–7.
13. Flynn JH. The 'temperature integral'—its use and abuse. Thermochim Acta. 1997;300:83–92.
14. Vyazovkin S, Dollimore D. Linear and nonlinear procedures in isoconversional computations of the activation energy of thermally induced reactions in solids. J Chem Inf Comput Sci. 1996;36:42–5.
15. APEX 2, SADABS and SAINT, Bruker AXS Inc., Madison, Wisconsin, USA; 2010.
16. Sheldrick GM. A short history of SHELX. Acta Crystallogr. 2008;A64:112–22.
17. Hübschle CB, Sheldrick GM, Dittrich B. ShelXle: a Qt graphical user interface for SHELXL. J Appl Crystallogr. 2011;44:1281–4.
18. Bērziņš A, Actiņš A. Effect of experimental and sample factors on dehydration kinetics of mildronate dihydrate: mechanism of dehydration and determination of kinetic parameters. J Pharm Sci. 2014;103:1747–55.
19. Aucamp M, Liebenberg W, Strydom SJ, van Tonder EC, de Villiers MM. Physicochemical properties of amorphous roxithromycin prepared by quench cooling of the melt or desolvation of a chloroform solvate. AAPS PharmSciTech. 2012;13:467–76.
20. Sánchez-Jiménez PE, Perejón A, Pérez-Maqueda LA, Criado JM. New insights on the kinetic analysis of isothermal data: the independence of the activation energy from the assumed kinetic model. Energy Fuels. 2015;29:392–7.
21. Khawam A, Flanagan DR. Solid-state kinetic models: basics and mathematical fundamentals. J Phys Chem B. 2006;110:17315–28.
22. Gotor FJ, Criado JM, Malek J, Koga N. Kinetic analysis of solid-state reactions: the universality of master plots for analysing isothermal and nonisothermal experiments. J Phys Chem A. 2000;104:10777–82.
23. Bachet B, Brassy C, Mornon JP. [*O*-(dioxa-2,5 hexyl) oxime]-9 de l'érythromycine A hydrate. Acta Crystallogr. 1988;C44: 112–6.
24. Holstein JJ, Luger P, Kalinowski R, Mebs S, Paulman C, Dittrich B. Validation of experimental charge densities: refinement of the macrolide antibiotic roxithromycin. Acta Crystallogr. 2010;B66:568–77.
25. Macrae CF, Bruno IJ, Chisholm JA, Edgington PR, McCabe P, Pidcock E, Rodriguez-Monge L, Taylor R, van der Streek J, Wood PA. Mercury CSD2.0—new features for the visualization and investigation of crystal structures. J Appl Crystallogr. 2008;41:466–70.
26. Koga N, Criado JM. Kinetic analyses of solid-state reactions with a particle-size distribution. J Am Ceram Soc. 1998;81:2901–9.